Modeling of Passively Synchronized Dual Wavelength *Q*-Switched Nd^{3+}:YVO_4 Lasers

B. Abdul Ghani* and M. Hammadi
Atomic Energy Commission, P.O. Box 6091, Damascus, Syria

(Received June 1, 2011; in final form January 16, 2012)

A mathematical model describing the sum frequency generation of passively synchronized *Q*-switched pulses simultaneously emitted from two separate Nd^{3+}:YVO_4 lasers has been demonstrated. This model describes the temporal behavior of the output pulses, and studies the impact of the pumping energy variation on the characteristics of these pulses (output power, pulse separation, pulse widths, delay time). V^{3+}:YAG and Cr^{4+}:YAG saturable absorbers and a periodically poled KTP crystal are used to achieve and improve the synchronization of the emitted 1342 nm and 1064 nm wavelengths. The synchronization process generates pulsed yellow light with 593.5 nm wavelength, and it can be realized through adjusting the pumping energy of the gain media.

PACS: 42.55.Rz, 42.60.Gd, 87.19.lm

1. Introduction

Low cost and compact are means of generating short and high-power laser pulses in the infrared spectral region and can be usually achieved using passive *Q*-switching process. Many passive *Q*-switches using Cr^{4+}:YAG crystal are efficient elements at 800–1200 nm wavelength range, while *Q*-switches using V^{3+}:YAG crystal are efficient elements at 1000–1500 nm wavelength range. The synchronization of laser pulses facilitates the sum/difference frequency mixing used in conversion long/short wave radiation [1].

Lasers in the yellow spectral region have found an increasing number of applications in bio-instrumentation, spectroscopy, dermatology, microscopy and other applications in different branches of science and technology. In the field of biomedical optics there is a great need for light sources operating in pulsed regime due to the high absorption in hemoglobin [2].

Previous studies of V^{3+}:YAG crystals showed that the V^{3+} ions can occupy both tetrahedral and octahedral coordinated positions [3]. Peaks at 800, 1140, and 1320 nm on the $^3A_2 \rightarrow {}^3T_1(^3F)$, $^3A_2 \rightarrow {}^1E(^1D)$ and $^3A_2 \rightarrow {}^3T_2(^3F)$ transitions can be attributed to tetrahedral. Therefore, this coordination of the ions is important for action of a passive *Q*-switch at 1064 nm and 1342 nm.

Synchronized *Q*-switched pulses can be obtained in two ways; either the two lasers shown in Fig. 1 must be able to generate independent *Q*-switched pulses, if they are pumped separately, and their repetition rates must be similar in order to synchronize properly; or one laser can be just below threshold and only being able to exceed threshold when the saturable absorber is bleached by the second laser [1, 4, 5]. Laser pulses must be synchronized very carefully in order to obtain efficient conversion in the nonlinear process, which leads to good understanding of the sum frequency generation (SFG) mechanism. Very stable passive synchronized *Q*-switching at two different wavelengths has been achieved by adjusting the pump power and improving the *Q*-switched behavior of the 1064 nm laser. This can be obtained by inserting an additional Cr^{4+}:YAG saturable absorber in the laser cavity.

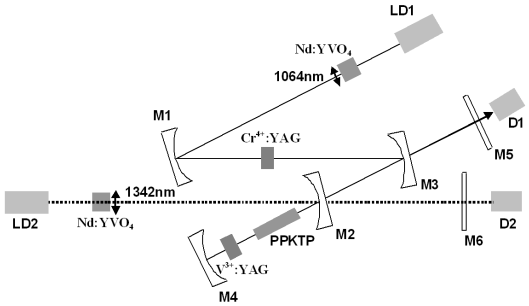

Fig. 1. Experimental setup of passively synchronized of two Nd^{3+}:YVO_4 lasers *Q*-switched with V^{3+}:YAG, Cr^{4+}:YAG/PPKTP saturable absorbers [2, 4].

The investigation of passively synchronized *Q*-switched Nd^{3+}:YVO_4 dual-wavelengths (1342 and 1064 nm) using V^{3+}:YAG or V^{3+}:YAG and Cr^{4+}:YAG saturable absorbers has been studied in many references [2, 4, 6]. The reported mathematical models in these references did not fully describe the *Q*-switched and SFG processes (593.5 nm).

This work focuses on the development of a mathematical model for investigating the SFG of passively synchronized *Q*-switched pulses emitted from two Nd^{3+}:YVO_4 lasers using V^{3+}:YAG or V^{3+}:YAG and Cr^{4+}:YAG saturable absorbers with PPKTP. The mathematical model,

* corresponding author; e-mail: pscientific@aec.org.sy

developed in this work, estimates the temporal behavior of the output pulses of the studied laser system.

2. Mathematical model

The mathematical model, developed in this work, describes the pulsed Nd^{3+}:YVO_4 pumping laser sources with V^{3+}:YAG or with both V^{3+}:YAG and Cr^{4+}:YAG solid-state saturable absorbers. It also investigates the synchronization of the emitted laser pulses and the SFG process [2, 4, 6–8].

2.1. Rate equations of laser media

The studied laser system, shown in Fig. 1, can be described by four coupled rate equations. These equations describe the population inversion and the laser density of the two synchronized Q-switched first (1342 nm) and second (1064 nm) laser fields. The system of equations takes into consideration the sum frequency mixing process, focusing, bleaching and one-directional propagation effects. The saturable absorber might be V^{3+}:YAG crystal only or V^{3+}:YAG and Cr^{4+}:YAG crystals together (Fig. 1).

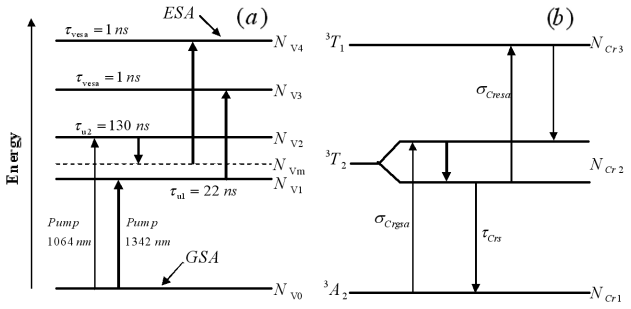

Fig. 2. Simple energy levels diagram for (a) V^{3+}:YAG and (b) Cr^{4+}:YAG saturable absorbers [2, 4, 8].

The time evolution of the population inversion and the laser densities of the laser fields are given by the following two equations (case of V^{3+}:YAG crystal only, Fig. 2a) [2, 4, 6–8]:

$$\frac{\mathrm{d}N_i}{\mathrm{d}t} = G_i - \frac{N_i}{\tau_{spi}} - 2\sigma_i v_{gi} N_i U_{Qi}, \tag{1}$$

$$\begin{aligned}\frac{\mathrm{d}U_{Qi}}{\mathrm{d}t} &= \mu_{gi}\sigma_i v_{gi} N_i U_{Qi} - \frac{U_{Qi}}{\tau_{pi}} + \Gamma\Omega\frac{N_i}{\tau_{spi}} \\ &- v_{si}\mu_{si}\Big\{\sigma_{gsai}\big[(2-i)N_{V1} + (i-1)N_{Vm} - N_{V0}\big] \\ &+ \sigma_{esai}\big[N_{V(i+2)} + (i-2)N_{V1} + (1-i)N_{Vm}\big]\Big\}U_{Qi} \\ &- \mu_{ki}\eta_{\mathrm{SFG}} W_{Pi}\prod_{i=1}^{2} U_{Qi},\end{aligned} \tag{2}$$

where $i = 1$ and 2 corresponds to the first and second laser fields with 1342 nm and 1064 nm wavelengths, respectively, $G_i = \eta_{pi}\frac{E_i^{\mathrm{T}}}{W_p}\frac{1}{t_0 V_{Ci}}\sqrt{F_i/\pi}\exp\left(-F_i\left(\frac{t}{t_0}-1\right)^2\right)$ [5, 9] is the pumping rate (considered to be a Gaussian function with its temporal peak at t_0, assuming that the pump is uniform over the whole crystal), η_{pi} is the total pumping efficiency, E_i^{T} is the total pumping energy, W_p is the diode pumping photon energy (at wavelength 808 nm), t_0 is the time of temporal peaks (in calculation t_0 is set to be approximately equal to the lifetime of the upper and higher state of the two different saturable absorbers), $V_{Ci} = \ell_{ci}A_i$ is the crystal's pumped volume, ℓ_{ci} is the length of the pumped Nd^{3+}:YVO_4 crystal, A_i is the cross-sectional area of the pumped Nd^{3+}:YVO_4 crystal, F_i is introduced to control the width of the pumping pulse, τ_{spi} is the spontaneous lifetime of the corresponding laser field, σ_i is the transition cross-section of the active medium for the emitted wavelength, $v_{gi} = c/n_{gi}$ is the light velocity in the gain medium, $v_{si} = c/n_{si}$ is the light velocity in saturable absorber, n_{gi}, n_{si} are the refractive indices in gain and saturable absorber media, respectively, $\mu_{gi} = n_{gi}\ell_{ci}/L_{ri}$, $\mu_{si} = n_{si}\ell_{sV}/L_{ri}$ and $\mu_{ki} = n_{ki}\ell_k/L_{ri}$ are the filling factors of the gain medium, saturable absorber medium and periodically poled KTP (PPKTP) crystal, respectively, ℓ_{sV} is the length of the V^{3+}:YAG saturable absorber, ℓ_k is the length of the KTP crystal.

$L_{ri} = [n_{gi}\ell_{ci} + n_{si}\ell_{sV} + n_{ki}\ell_k + (L_{cavi} - \ell_{ci} - \ell_{sV} - \ell_k)]$ is the optical resonator length, L_{cavi} is the length of the laser cavity, $\tau_{pi} = \tau_{cavi}/\rho_{lossi}$ is the photons' lifetime, $\tau_{cavi} = 2L_{ri}/c$ is the round trip time cavities, c is the light velocity, $\rho_{lossi} = \rho_{\mathrm{passi}} + \rho_{Ti} + \rho_{si}$ is the total dynamic round trip losses, ρ_{passi} is the round trip loss, ρ_{Ti} is the transmission of the output coupler, ρ_{si} is the saturable absorber losses, Γ is the confinement factor, Ω is the solid angle, σ_{gsai}, σ_{esai} is the cross-section of the ground and excited-state absorption of the laser field, respectively, N_{V0}, N_{V1}, N_{Vm} are the population inversion of the ground, first excited and extra levels of V^{3+}:YAG crystal, N_{V3}, N_{V4} are the population inversion of the higher excited levels [2, 4].

Assuming infinite plane wave, non-depleted pump approximation, small signal approximation, uniformly spatial intensity distribution, and weak coupling case, the coupling coefficient of the SFG process is given as follows [2, 10]:

$$\eta_{\mathrm{SFG}} = 2\eta_0^3\varepsilon_0^2\omega_{\mathrm{SFG}}^2\frac{d_{\mathrm{eff}}^2 L_K A}{n_{k1}n_{k2}n_{\mathrm{SFG}}}\mathrm{sinc}^2(\Delta K L_K/2),$$

where $\eta_0 = \sqrt{\mu_0/\varepsilon_0}$ is the impedance of free space (μ_0 is the magnetic permeability of vacuum and ε_0 is the dielectric permittivity of vacuum), ω_{SFG} is the frequency of SFG wavelength, d_{eff} is the effective second order nonlinear coefficient (electric dipole moment of KTP crystal), A is the cross-sectional area of interacting waves, n_{SFG} is the refractive index of SFG in PPKTP crystal (593.5 nm), $\mathrm{sinc}^2(\Delta k L_k/2)$ introduces the effect of phase mismatch in the efficiency of the SFG process, $\Delta k = 2\pi\left(\frac{n_{\mathrm{SFG}}}{\lambda_{\mathrm{SFG}}} - \frac{n_{1k}}{\lambda_{p1}} - \frac{n_{2k}}{\lambda_{p2}}\right)$ is the phase mismatch [2], λ_{Pi} is the wavelength of the first and second laser fields, respectively and W_{Pi} is the lasing photon energy of the laser fields.

It should be mentioned here that in case of having two saturable absorbers (V^{3+}:YAG and Cr^{4+}:YAG), Eq. (2) for the second laser field ($i = 2$) becomes as follows (Fig. 2b):

$$\frac{\mathrm{d}U_{Q2}}{\mathrm{d}t} = \mu_{g2}\sigma_2 v_{g2} N_2 U_{Q2} - \frac{U_{Q2}}{\tau_{p2}} + \Gamma\Omega\frac{N_2}{\tau_{sp2}} - v_{s2}\mu_{s2}\big[\sigma_{\mathrm{Cr}gsa}(N_{\mathrm{Cr}2} - N_{\mathrm{Cr}1}) + \sigma_{\mathrm{Cr}esa}(N_{\mathrm{Cr}3} - N_{\mathrm{Cr}2})\big]U_{Q2} - \mu_{k2}\eta_{\mathrm{SFG}} W_{f2}\prod_{i=1}^{2} U_{Qi}. \quad (2^*)$$

By considering the bidirectional propagation, the output laser power for passively synchronized Q-switched laser fields is given by the following relation ($i = 1$ for 1342 nm and $i = 2$ for 1064 nm wavelengths):

$$P_i = A_i W_{fi} c U_{Qi}\delta_i/2n_{gi}, \quad (3)$$

where $\delta_i = 1 - |R_{2i}|^2$ represents the impact of the Q-switching process and $A_i = \pi w_{0i}^2/4$ is the area of the spot size of pumping wavelength.

Assuming that the KTP is periodically poled to N_w waveguide with the period of 12.65 μm, then the SFG power is given by the following relation [11, 12]:

$$P_s = \eta_{\mathrm{SFG}}(N_w)^2 P_1(0) P_2/A, \quad (4)$$

where $P_1(0)$ is the pumping power.

2.2. V^{3+}:YAG saturable absorber rate equations

The V^{3+}:YAG saturable absorber operating at 1342 nm and 1064 nm wavelengths can be characterized by the simple energy levels diagram shown in Fig. 2a. The important transitions are taking place between ground state N_{V0} and energy levels N_{V1} and N_{V2} for absorbing wavelength of 1342 nm and 1064 nm, respectively.

The time evolution of the population inversion of the ground state of V^{3+}:YAG crystal for the first ($i = 1$) and second ($i = 2$) optical laser fields coupled through saturation effect is given as follows [2, 4, 7]:

$$\frac{\mathrm{d}N_{V0}}{\mathrm{d}t} = -2v_{s1}(N_{V0} - N_{V1})\sigma_{gsa1}U_{Q1}\frac{w_{b1}}{w_{01}} - 2v_{s2}(N_{V0} - N_{Vm})\sigma_{gsa2}U_{Q2}\frac{w_{b2}}{w_{02}} + \frac{N_{V1} + N_{Vm}}{\tau_{u1}}, \quad (5)$$

where w_{bi} is the beam waist of pumping diode laser at the Nd^{3+}:YVO_4 laser, w_{0i} is the beam waist of the emitted Nd^{3+}:YVO_4 at the saturable absorber crystal, τ_{u1} is the lifetime of the first excited level for 1342 nm wavelength (Fig. 2a).

The time evolution of the population inversion of the first excited level of V^{3+}:YAG crystal for first and second optical laser fields is given by the following two equations [2, 4, 6, 7]:

$$\frac{\mathrm{d}N_{V1}}{\mathrm{d}t} = 2v_{s1}(N_{V0} - N_{V1})\sigma_{gsa1}U_{Q1}\frac{w_{b1}}{w_{01}} - 2v_{s1}(N_{V1} - N_{V3})\sigma_{esa1}U_{Q1}\frac{w_{b1}}{w_{01}} + \frac{N_{V1}}{\tau_{u1}} + \frac{N_{V3}}{\tau_{esa}}, \quad (6)$$

$$\frac{\mathrm{d}N_{V2}}{\mathrm{d}t} = 2v_{s2}(N_{V0} - N_{V2})\sigma_{gsa2}U_{Q2}\frac{w_{b2}}{w_{02}} - \frac{N_{V2}}{\tau_{u2}}, \quad (7)$$

where τ_{u2} is the lifetime of the first excited level for 1064 nm wavelength and τ_{esa} is the relaxation time of higher excited state (Fig. 2a) [2, 4, 6, 7].

The time evolution of the population inversion of the higher excited levels of the V^{3+}:YAG crystal is given by the following two equations [2, 4, 6, 7]:

$$\frac{\mathrm{d}N_{V3}}{\mathrm{d}t} = 2v_{s1}(N_{V1} - N_{V3})\sigma_{esa1}U_{Q1}\frac{w_{b1}}{w_{01}} - \frac{N_{V3}}{\tau_{esa}}, \quad (8)$$

$$\frac{\mathrm{d}N_{V4}}{\mathrm{d}t} = 2v_{s2}(N_{Vm} - N_{V4})\sigma_{esa2}U_{Q2}\frac{w_{b2}}{w_{02}} - \frac{N_{V4}}{\tau_{esa}}. \quad (9)$$

The Boltzmann distribution of the broad band of vibronic energy levels of the V^{3+} ions requires the existence of extra level N_{Vm} (Fig. 2a), to whom decay atoms from level N_{V2} without perturbing the population of the energy level N_{V1} [2, 7].

The time evolution of the population inversion of extra level N_{Vm} of V^{3+}:YAG crystal for the second laser field is given as follows [2, 4, 6, 7]:

$$\frac{\mathrm{d}N_{Vm}}{\mathrm{d}t} = -2v_{s2}(N_{Vm} - N_{V4})\sigma_{esa2}U_{Q2}\frac{w_{b2}}{w_{02}} + \frac{N_{V2}}{\tau_{u2}} + \frac{N_{V4}}{\tau_{esa}} - \frac{N_{Vm}}{\tau_{u1}}. \quad (10)$$

2.3. Cr^{4+}:YAG saturable absorber rate equations

Free Cr^{4+} ions ^3F state, as well known, splits into three states $^3A_2$, $^3T_2$ and $^3T_1$ (Fig. 2b). It is assumed that the phonons relaxation within the different manifolds is infinitely fast, so only the states $N_{\mathrm{Cr}1}, N_{\mathrm{Cr}2}, N_{\mathrm{Cr}3}$ are populated [8, 13].

The time evolution of population density of the ground state of Cr^{4+}:YAG crystal $^3A_2$ for the second laser field is given by the following relation (Fig. 2b) [8]:

$$\frac{\mathrm{d}N_{\mathrm{Cr}1}}{\mathrm{d}t} = -\sigma_{\mathrm{Cr}gsa}v_{s2}\frac{w_{b2}}{w_{02}}U_{Q2}N_{\mathrm{Cr}1} + \frac{N_{\mathrm{Cr}2}}{\tau_{\mathrm{Cr}U}} + \frac{N_{\mathrm{Cr}2}}{\tau_{\mathrm{Cr}s}}. \quad (11)$$

The time evolution of the population density of the first excited state $^3T_2$ of Cr^{4+}:YAG crystal, for the second laser field, is given by the following relation [8]:

$$\frac{\mathrm{d}N_{\mathrm{Cr}2}}{\mathrm{d}t} = \sigma_{\mathrm{Cr}gsa}v_{s2}\frac{w_{b2}}{w_{02}}U_{Q2}N_{\mathrm{Cr}1} + \sigma_{\mathrm{Cr}esa}v_{s2}\frac{w_{b2}}{w_{02}}U_{Q2}(N_{\mathrm{Cr}3} - N_{\mathrm{Cr}2}) - \frac{N_{\mathrm{Cr}2}}{\tau_{\mathrm{Cr}U}} - \frac{N_{\mathrm{Cr}2}}{\tau_{\mathrm{Cr}s}} + \frac{N_{\mathrm{Cr}3}}{\tau_{\mathrm{Cr}esa}}. \quad (12)$$

The time evolution of the population density of the higher excited state $^3T_1$ of Cr^{4+}:YAG crystal, for the second laser field, is given by the following relation [8]:

$$\frac{\mathrm{d}N_{\mathrm{Cr}3}}{\mathrm{d}t} = -\sigma_{\mathrm{Cr}esa}v_{s2}\frac{w_{b2}}{w_{02}}U_{Q2}(N_{\mathrm{Cr}3} - N_{\mathrm{Cr}2}) - \frac{N_{\mathrm{Cr}3}}{\tau_{\mathrm{Cr}esa}}, \quad (13)$$

where $\sigma_{\mathrm{Cr}gsa}$ and $\sigma_{\mathrm{Cr}esa}$ are the ground and excited state absorption cross-section of Cr^{4+}:YAG crystal, respectively, $\tau_{\mathrm{Cr}U}$ is the lifetime of the upper level $^3T_2$, $\tau_{\mathrm{Cr}s}$ is

the radiative lifetime of the spontaneous emission, $\tau_{\mathrm{Cr}esa}$ is the relaxation time of higher excited state $^3T_1$.

3. Numerical solution of rate equations

The rate Eqs. (1), (2), (5)–(10) and (1), (2), (5), (6), (8), (11)–(13) represent two systems of stiff ordinary nonlinear differential equations. These equations describe the intracavity dual wavelength SFG of passively synchronized Q-switched laser system using V^3:YAG, V^{3+}:YAG and Cr^{4+}:YAG, respectively as saturable absorber with PPKTP.

A computer program, based on a variable time-step fourth-order Runge–Kutta subroutine has been used for simulation. This computer program allows the investigation of the influence of the variation of the pumped diode laser energies of Nd^{3+}:YVO_4/V^{3+}:YAG/KTP and Nd^{3+}:YVO_4/V^{3+}:YAG/Cr^{4+}:YAG/KTP laser fields on the SFG of a Q-switched output laser pulse characteristics (output power, pulse separation, delay time and build up time).

The physical constants and geometrical parameters of passively synchronized Q-switched laser fields of the rate equations are given in Table [1, 2, 4, 5, 8–14].

TABLE

Physical constants and geometrical parameters of the passively synchronized dual wavelength diode-pumped of a Q-switched Nd^{3+}:YVO_4 lasers based on V^{3+}:YAG and Cr^{4+}:YAG solid state saturable absorbers.

Constant	Value	Unit	Constant	Value	Unit
τ_{sp1}	90×10^{-6}	s	L_{Cav2}	56	cm
τ_{sp2}	90×10^{-6}	s	ℓ_{C1}	0.3	cm
σ_1	7.6×10^{-19}	cm^2	ℓ_{C2}	0.3	cm
σ_2	16×10^{-19}	cm^2	ℓ_{sv}	0.05	cm
τ_{u1}	22×10^{-9}	s	ℓ_{scr}	0.1	cm
τ_{u2}	130×10^{-12}	s	ρ_{pass1}	2	%
τ_{esa}	1×10^{-9}	s	ρ_{pass2}	4	%
σ_{gsa1}	7.2×10^{-18}	cm^2	ρ_{T1}	0.1	%
σ_{gsa2}	3.0×10^{-18}	cm^2	ρ_{T2}	0.1	%
σ_{esa1}	7.4×10^{-19}	cm^2	$\tau_{\mathrm{Cr}s}$	30.6×10^{-6}	s
σ_{esa2}	1.4×10^{-19}	cm^2	$\tau_{\mathrm{Cr}U}$	3×10^{-6}	s
$\sigma_{\mathrm{Cr}gsa}$	5.7×10^{-18}	cm^2	$\tau_{\mathrm{Cr}esa}$	10×10^{-12}	s
$\sigma_{\mathrm{Cr}esa}$	8.0×10^{-19}	cm^2	ℓ_k	0.9	cm
W_{p1}	1.478×10^{-19}	J	d_{eff}	7.6×10^{-10}	cm/V
W_{p2}	1.86×10^{-19}	J	ε_0	8.85×10^{-14}	F/cm
W_{sf}	3.432×10^{-19}	J	N_w	712	–
Γ	0.35	–	L_{Cav1}	20	cm
Ω	1×10^{-3}	–			

The initial values of the rate equations have been chosen as follows: $N_{V0} = 2.778 \times 10^{17}$ [1/cm^3], $N_{V1} = 0.0$ [1/cm^3], $N_{V2} = 0.0$ [1/cm^3], $N_{V3} = 0.0$ [1/cm^3], $N_{V4} = 0.0$ [1/cm^3], $N_{Vm} = 0.0$ [1/cm^3], $N_{\mathrm{Cr}1} = 1.754 \times 10^{17}$ [1/cm^3], $N_{\mathrm{Cr}2} = N_{\mathrm{Cr}3} = 0.0$ [1/cm^3], $N_i = N_{th.i} = \frac{(\rho_{\mathrm{passi}})+(\rho_s)_i+(\rho_{\mathrm{T}})_i}{2\sigma_i(\ell_c)_i}$ $(i = 1, 2)$, $U_{Q1} = 10^{-9}$ [1/cm^3], $U_{Q2} = 10^{-9}$ [1/cm^3], $(\rho_{s1} = 2(N_{V0} - N_{V1})\ell_{sV}\sigma_{gsa1}$, $\rho_{s2} = 2(N_{V0}-N_{V1})\ell_{sV}\sigma_{gsa2}+2(N_{\mathrm{Cr}0}-N_{\mathrm{Cr}1})\ell_{s\mathrm{Cr}}\sigma_{gsa\mathrm{Cr}})$, where $N_{th.i}$ is the threshold population inversion and $\ell_{s\mathrm{Cr}}$ is the length of the Cr^{4+}:YAG saturable absorber.

4. Results and discussion

Figure 3 shows the temporal behavior of the population inversion density of laser fields for $\langle 1 \rangle$ first laser field (1342 nm) and $\langle 2 \rangle$ second laser field (1064 nm) using: (a) V^{3+}:YAG and Cr^{4+}:YAG saturable absorbers and (b) V^{3+}:YAG saturable absorber.

Figure 3a is obtained for pumping power of 2 W and 4 W for the 1342 nm and 1064 nm laser fields, respectively, while Fig. 3b is obtained for pumping powers equal to 2 W and 4.5 W. It can be noticed from both figures that the cavity losses saturated during the first 60 ns. The population inversion starts decreasing as the passive losses exceed the gain. The mismatch between the pumping power thresholds is due to the differences between the absorption saturable losses in the laser cavity. The deep depletion of the 1064 nm ground state population (Fig. 3b) is due to the significant short recovery time of the V^{3+}:YAG in comparison with the Cr^{4+}:YAG saturable absorber. Due to the strong field at the 1342 nm transition, the losses of 1342 nm and 1064 nm wavelengths saturate at the same time. After that, the gain exceeds the losses and the lasers start oscillating. The behavior of this process can occur periodically.

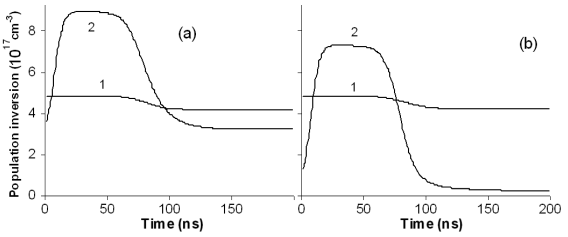

Fig. 3. Temporal behavior of the population inversion density of laser fields for ⟨1⟩1342 nm and ⟨2⟩1064 nm wavelengths using: (a) V^{3+}:YAG and Cr^{4+}:YAG saturable absorbers; (b) V^{3+}:YAG saturable absorber.

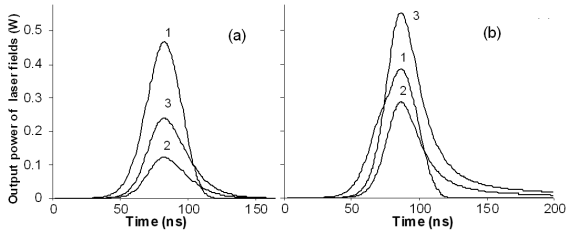

Fig. 4. Temporal behavior of passively synchronized Q-switched output laser power; ⟨1⟩1342 nm, ⟨2⟩1064 nm and ⟨3⟩593.5 nm (SFG) laser fields using: (a) V^{3+}:YAG and Cr^{4+}:YAG saturable absorbers with 2 W of pump power for 1342 nm laser field and 4 W for 1064 nm laser field; (b) V^{3+}:YAG saturable absorber with 2 W of pump power for 1342 nm laser field and 4.5 W for 1064 nm laser field.

Figure 4 shows the temporal behavior of the passively synchronized Q-switched output power of laser pulses; ⟨1⟩1342 nm, ⟨2⟩1064 nm and ⟨3⟩593.5 nm (SFG) laser fields using (a) V^{3+}:YAG and Cr^{4+}:YAG saturable absorbers with 2 W of pump power for 1342 nm laser field and 4 W for 1064 nm laser field and (b) V^{3+}:YAG saturable absorber with 2 W of pump power for 1342 nm laser field and 4.5 W for 1064 nm laser field. The Cr^{4+}:YAG ground-state absorption cross-section at 1064 nm is almost twice higher than the V^{3+}:YAG cross--section. Using the Cr^{4+}:YAG crystal as an additional saturable absorber allows generating output pulses at 1064 nm of repetition rate similar to the repetition rate of 1342 nm laser. This may generates better synchronized Q-switched pulses. For 6 W of total pump power of both lasers in case of V^{3+}:YAG and Cr^{4+}:YAG saturable absorbers, the optical efficiency for the SFG process reaches 40%, while it is 11% in [2].

Figures 5 and 6 show the changes in the delay time and pulse separation between the output 1342 nm and 1064 nm pulses by changing the pump power of the 1064 nm laser and fixing the 1342 nm laser power. It can be seen from these two figures that, for both laser fields, the variation of the 1064 nm pump power leads to different positions of the output peak pulse in comparison with the fixed position of the 1342 nm peak pulse. Full synchronization (repetition rate of 1064 nm matches

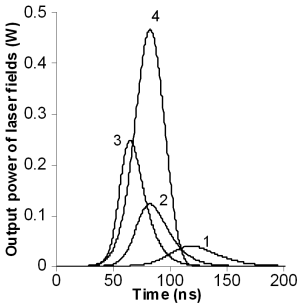

Fig. 5. Changes in the delay time between two emitted pulses of 1342 nm and 1064 nm, by changing the pump power of the 1064 nm (⟨1⟩2 W, ⟨2⟩4 W and ⟨3⟩6 W) using V^{3+}:YAG and Cr^{4+}:YAG saturable absorbers. The 1342 nm laser is fixed at 2 W of pump power (curve 4).

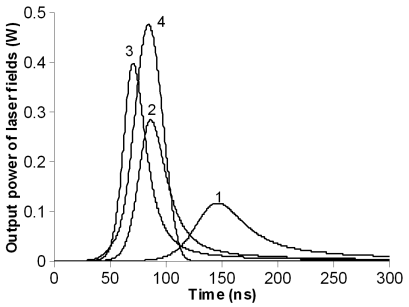

Fig. 6. Changes in the delay time between two emitted pulses of 1342 nm and 1064 nm, by changing the pump power of the 1064 nm (⟨1⟩2 W, ⟨2⟩4.5 W and ⟨3⟩6 W) using V^{3+}:YAG saturable absorber. The 1342 nm laser is fixed at 2 W of pump power (curve 4).

the repetition rate of 1342 nm) between these two pulses can be reached for 4 W of the pump power (curve ⟨2⟩) in case of using V^{3+}:YAG and Cr^{4+}:YAG saturable absorbers (Fig. 5) and for 4.5 W (curve ⟨2⟩) in case of using V^{3+}:YAG saturable absorber only (Fig. 6). By increasing the pump power to a value more than 6 W, the overlap between the two pulses is gradually eliminated. It can also be noticed from Figs. 5 and 6 that the pulse separation of 1064 nm pulses (⟨1⟩, ⟨2⟩ and ⟨3⟩) is changing nonlinearly by changing the 1064 nm pump power.

5. Conclusion

A mathematical model describing the intracavity dual wavelength sum frequency generation of two passively synchronized Q-switched Nd^{3+}:YVO_4 laser pulses has been developed. The synchronization process of the two Q-switched 1342 nm and 1064 nm laser fields with a periodically poled KTP crystal leads to a new pulsed solid state 593.5 nm yellow light source.

The synchronization process can be realized by adjusting the pump power of the Nd^{3+}:YVO_4 laser systems. It is found that to improve the Q-switched behavior of the 1064 nm laser, an additional Cr^{4+}:YAG saturable ab-

sorber should be inserted into the system next to the V^{3+}:YAG crystal. This leads to obtain similar repetition rates at the two wavelengths and get stable state of synchronization.

Acknowledgments

The authors would like to express their thanks to the Director General of AECS Prof. I. Othman for his continuous encouragement, guidance, and support.

References

[1] P. Tidemand-Lichtenberg, J. Janousek, R. Melich, J.L. Mortensen, P. Buchhave, *Opt. Commun.* **241**, 487 (2004).

[2] J. Janousek, M.Sc. Thesis 2004.

[3] A.M. Malyarevich, I.A. Denisov, K.V. Yumashev, V.P. Mikhailov, R.S. Conroy, B.D. Sinclair, *Appl. Phys. B* **67**, 555 (1998).

[4] J. Janousek, P. Tidemand-Lichtenberg, J.L. Mortensen, P. Buchave, *Opt. Commun.* **265**, 277 (2006).

[5] H. Su, H, H. Shen, W.X. Lin, R.R. Zeng, C.H. Huang, G. Zhang, *J. Appl. Phys.* **84**, 6519 (1998).

[6] Y.F. Chen, Y.S. Chen, S.W. Tsai, *Appl. Phys. B* **79**, 207 (2004).

[7] Y.F. Chen, S.W. Tsai, *Opt. Lett.* **27**, 397 (2002).

[8] B. Abdul Ghani, M. Hammadi, *J. Opt. A, Pure Appl. Opt.* **8**, 229 (2006).

[9] G.A. Henderson, *J. Appl. Phys.* **68**, 5451 (1990).

[10] R.L. Sutherland, *Handbook of Nonlinear Optics*, Marcel Dekker, Inc. 1996.

[11] B. Abdul Ghani, M. Hammadi, *J. Opt. A, Pure Appl. Opt.* **11**, 105504 (2009).

[12] W. Koechner, *Solid-State Laser Engineering*, 6th ed., Springer Verlag, Berlin 2005.

[13] C.W. Wang, Y.L. Weng, P.L. Huang, H.Z. Cheng, S.L. Huang, *Appl. Opt.* **41**, 1075 (2002).

[14] K. Fradkin, A. Arie, A. Skliar, G. Rosenman, *Appl. Phys. Lett.* **74**, 914 (1999).